High-Precision Quantum-Enhanced Gravimetry with a Bose-Einstein Condensate

Stuart S. Szigeti,[1,*] Samuel P. Nolan,[2] John D. Close,[1] and Simon A. Haine[1]
[1] *Department of Quantum Science, Research School of Physics, The Australian National University, Canberra 2601, Australia*
[2] *QSTAR, INO-CNR and LENS, Largo Enrico Fermi 2, Firenze 50125, Italy*

(Received 1 May 2020; accepted 27 July 2020; published 3 September 2020)

We show that the inherently large interatomic interactions of a Bose-Einstein condensate (BEC) can enhance the sensitivity of a high precision cold-atom gravimeter beyond the shot-noise limit (SNL). Through detailed numerical simulation, we demonstrate that our scheme produces spin-squeezed states with variances up to 14 dB below the SNL, and that absolute gravimetry measurement sensitivities between two and five times below the SNL are achievable with BECs between 10^4 and 10^6 in atom number. Our scheme is robust to phase diffusion, imperfect atom counting, and shot-to-shot variations in atom number and laser intensity. Our proposal is immediately achievable in current laboratories, since it needs only a small modification to existing state-of-the-art experiments and does not require additional guiding potentials or optical cavities.

DOI: 10.1103/PhysRevLett.125.100402

Atom interferometers provide state-of-the-art measurements of gravity [1–7] and gravity gradiometry [8–13]. Future applications of cold-atom gravimetry are wide ranging [14], including inertial navigation [15–17], mineral exploration [18–20], groundwater monitoring [21], satellite gravimetry [22,23], and weak equivalence principle experiments that test candidate theories of quantum gravity [24–26]. These applications require significant improvements to cold-atom gravimeters: improved precision [27], increased stability [28], increased dynamic range [29], increased measurement rate [30], and decreased size, weight, and power (SWAP) [31–33].

Quantum entanglement offers a promising route to improved cold-atom gravimetry, since it enables relative-phase measurements below the shot-noise limit (SNL). Metrologically useful entanglement has been generated in large cold-atom ensembles via atom-atom [34–40] and atom-light interactions [41–44], with sub-shot-noise atom interferometry demonstrated in proof-of-principle experiments [45–51]. However, no quantum-enhanced (sub-shot-noise) atom interferometer has demonstrated *any* sensitivity to gravity, even in laboratory-based proof-of-principle apparatus. The key challenge is that most methods of generating entangled atomic states are incompatible with the stringent requirements of precision gravimetry. Cold-atom gravimeters require the creation and manipulation of well-defined and well-separated atomic matterwave momentum modes [52,53]. Although entanglement generation between internal atomic states is relatively mature, no experiment has shown that entanglement between internal states can be converted into entanglement between well-separated, controllable momentum modes suitable for gravimetry. There are promising proposals for creating squeezed momentum states for atom interferometry [54–57], however these require atom interferometry within an optical cavity which, whilst possible [58], is technically challenging and not always viable (e.g., low-SWAP scenarios). Even if entangled momentum states are available, this does not guarantee that they can be achieved with large atom number sources, nor that a high degree of coherence can be maintained between momentum modes for significant interrogation times.

In this Letter, we propose a quantum-enhanced ultracold-atom gravimetry scheme that operates in free space. Our scheme uses the large interatomic collisions of a Bose-Einstein condensate (BEC) to generate metrologically useful entanglement via one-axis twisting (OAT) [59,60], a nonlinear self-phase modulation that can reduce the relative number fluctuations between two well-defined momentum modes. It does not require additional guiding potentials or optical cavities, making it suitable for low-SWAP scenarios. Our scheme requires only a small modification to existing state-of-the-art experiments, so it is immediately achievable in current laboratories. We show that significant spin squeezing is attainable for large atom numbers and that this spin squeezing results in a useful improvement to absolute gravimetry sensitivity. We further show that our scheme is robust to phase diffusion and common experimental imperfections, including imperfect atom counting and shot-to-shot variations in atom number and laser intensity.

Gravimetry with a BEC.—Commonly, an atomic Mach-Zehnder (MZ) is used for gravimetry, where state-changing Raman transitions act as beam splitters ($\pi/2$ pulses) and mirrors (π pulses) [61]. Raman transitions, achieved with two counterpropagating laser pulses of wave vector $\mathbf{k}_L$, coherently couple two internal states $|1\rangle$ and $|2\rangle$. Transitions from $|1\rangle$ to $|2\rangle$ impart $2\hbar\mathbf{k}_L$ momentum to the atoms, giving the momentum separation needed for gravimetry. For N uncorrelated atoms a uniform gravitational acceleration can be measured with single-shot sensitivity $\Delta g = 1/(\sqrt{N} k_0 T^2)$, where k_0 is the component of $2\mathbf{k}_L$ aligned with gravity and T is the time between pulses (interrogation time) [61].

There are advantages to using BECs for precision gravimetry. A BEC's large coherence length and narrow momentum width enables high fringe contrast [7,62], improves the efficiency of large momentum transfer beam splitting [63,64], and mitigates many systematic and technical noise effects [65,66]. However, a BEC's large interatomic interactions are generally considered an unwanted hinderance. Interatomic collisions couple number fluctuations into phase fluctuations, causing phase diffusion, which degrades sensitivity [67,68]. Consequently, the effects of interatomic collisions are minimized by freely expanding the BEC prior to the MZ's first beam splitting pulse [Fig. 1(a)], which converts most of the collisional energy to kinetic energy. This reduces phase diffusion and gives excellent mode matching (required for high fringe contrast), since the BEC's spatial mode is largely preserved under free expansion [69,70].

Quantum-enhanced gravimetry with a BEC.—Our scheme, depicted in Fig. 1(b), is a modification of the standard MZ. Instead of "wasting" the strong interatomic interactions during this initial expansion period, our scheme exploits them with a "state-preparation" interferometer that generates spin squeezing via OAT. Representing the state as a Husimi-Q distribution on the Bloch sphere [71,72], OAT causes a shearing of the distribution [Fig. 1(c)]. The second beam splitter (BS2) rotates the distribution such that it is more sensitive to phase fluctuations within the interferometer, resulting in reduced relative number fluctuations at the output. Necessarily, BS2 is not a 50/50 beam splitter, with the relative population transfer dependent on the degree of squeezing. Unlike trapped schemes, where interatomic collisions cause unwanted multimode dynamics that make it difficult to match the two modes upon recombination [73], a BEC's spatial mode is almost perfectly preserved under free expansion, even for large atom numbers and collisional energies. The two modes are therefore well matched throughout the interferometer sequence. Furthermore, since the collisional energy is converted to kinetic energy during expansion, the interatomic interactions effectively "switch off" after $\sim$10 ms, minimizing their effect during most of the interferometer sequence. For $T \gg T_{\mathrm{OAT}}$, our scheme enables a gravity measurement with sensitivity [74]

$$\Delta g = \frac{\xi}{\sqrt{N} k_0 T^2} = \frac{1}{\sqrt{N} k_0 T^2} \min_{\theta,\phi} \left(\frac{N \mathrm{Var}(\hat{J}_{\theta,\phi})}{\langle \hat{J}_{\frac{\pi}{2},\phi+\frac{\pi}{2}} \rangle^2} \right)^{\frac{1}{2}}, \quad (1)$$

where $\xi \equiv \min_{\theta,\phi} \xi_{\theta,\phi}$ is the spin squeezing parameter [60,87] and $\hat{J}_{\theta,\phi} = \sin\theta \sin\phi \hat{J}_x + \sin\theta\cos\phi \hat{J}_y + \cos\theta \hat{J}_z$. Here $\hat{J}_i = \frac{1}{2}\int d\mathbf{r} \boldsymbol{\psi}^\dagger(\mathbf{r}) \boldsymbol{\sigma}_i \boldsymbol{\psi}(\mathbf{r})$ are pseudospin operators, where $\boldsymbol{\sigma}_i$ are the set of Pauli matrices, $\boldsymbol{\psi}(\mathbf{r}) = [\hat{\psi}_1(\mathbf{r}), \hat{\psi}_2(\mathbf{r}) e^{ik_0 z}]^T$ with $\hat{\psi}_1(\mathbf{r})$ and $\hat{\psi}_2(\mathbf{r})$ being field operators describing the BEC's two internal states $|1\rangle$ and $|2\rangle$, respectively, and $i = x,\ y,\ z$. Since $[\hat{\psi}_i(\mathbf{r}), \hat{\psi}_j^\dagger(\mathbf{r}')] = \delta_{ij}\delta(\mathbf{r}-\mathbf{r}')$, $[\hat{J}_i, \hat{J}_j] = i\epsilon_{ijk}\hat{J}_k$ with ϵ_{ijk} the Levi-Civita symbol. Physically, $\hat{J}_z$ is proportional to the population difference between the two internal states, whilst $\hat{J}_x$ and $\hat{J}_y$ encode coherences between the modes. Equation (1) shows that our scheme is capable of high precision, quantum-enhanced gravimetry provided $\xi < 1$, which is a sufficient condition for spin squeezing [88].

Analytic model of spin squeezing.—In what follows, we assume Raman pulse durations that are much shorter than the timescale for atomic motional dynamics. Typical atom interferometers operate in this regime, allowing us to treat the Raman coupling as an instantaneous beamsplitter unitary $\hat{U}_{\theta,\phi}$ [53]:

$$\hat{U}_{\theta,\phi}^\dagger \hat{\psi}_1 \hat{U}_{\theta,\phi} = \cos\left(\frac{\theta}{2}\right)\hat{\psi}_1 - ie^{i\phi}\sin\left(\frac{\theta}{2}\right)\hat{\psi}_2 e^{ik_0 z}, \quad (2a)$$

$$\hat{U}_{\theta,\phi}^\dagger \hat{\psi}_2 \hat{U}_{\theta,\phi} = \cos\left(\frac{\theta}{2}\right)\hat{\psi}_2 - ie^{-i\phi}\sin\left(\frac{\theta}{2}\right)\hat{\psi}_1 e^{-ik_0 z}, \quad (2b)$$

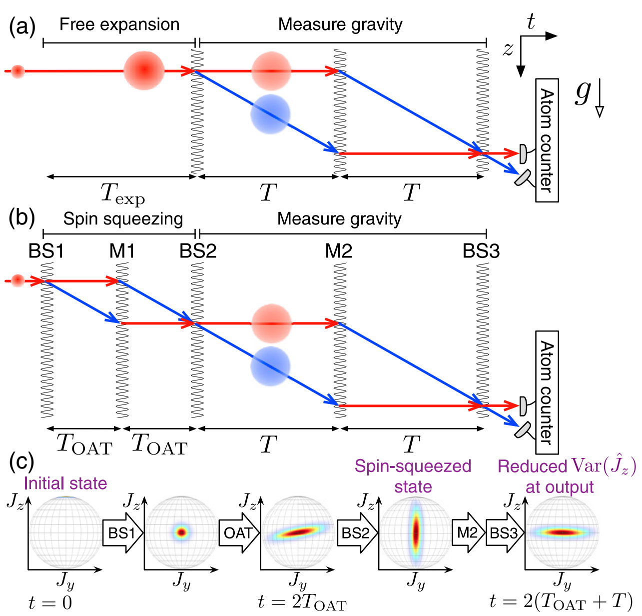

FIG. 1. (a) Space-time diagram illustrating SNL gravimetry with a BEC. Unwanted interatomic interactions are reduced by freely expanding the BEC for duration T_{exp}. A $\pi/2-\pi-\pi/2$ Raman pulse sequence then creates a MZ interferometer of interrogation time T. The two interferometer modes correspond to internal states $|1\rangle$ (red) and $|2\rangle$ (blue) with $\hbar k_0$ momentum separation. (b) Quantum-enhanced ultracold-atom gravimetry. During initial expansion duration $T_{\mathrm{exp}} = 2T_{\mathrm{OAT}}$, the BEC's interatomic interactions generate spin squeezing via OAT. (c) Bloch sphere representation of state during quantum-enhanced gravimetry.

where θ and ϕ are the beam splitting angle and phase, respectively.

Typical spin squeezing models approximate $\hat{\psi}_1(\mathbf{r}) \approx u_1(\mathbf{r})\hat{a}_1$ and $\hat{\psi}_2(\mathbf{r}) \approx u_2(\mathbf{r})e^{ik_0 z}\hat{a}_2$, where bosonic modes $\hat{a}_i$ correspond to the two interferometer paths [34]. This neglects the effect of imperfect spatial-mode overlap on the spin squeezing, which can be substantial [73]. Here, we assume $\hat{\psi}_1(\mathbf{r},t) = u_1(\mathbf{r},t)\hat{a}_1 + \hat{v}_1(\mathbf{r},t)$ and $\hat{\psi}_2(\mathbf{r},t) = u_2(\mathbf{r},t)e^{ik_0 z}\hat{a}_2 + \hat{v}_2(\mathbf{r},t)$, where $\int d\mathbf{r}|u_i(\mathbf{r},t)|^2 = 1$ and $\hat{v}_i(\mathbf{r},t)$ are "vacuum" operators satisfying $\hat{v}_i(\mathbf{r},t)|\Psi\rangle = 0$ and $[\hat{v}_i(\mathbf{r},t), \hat{v}_j^\dagger(\mathbf{r},t)] = \delta_{i,j}[\delta(\mathbf{r}-\mathbf{r}') - u_i(\mathbf{r},t)u_j^*(\mathbf{r}',t)]$ [75].

We calculate $\xi_{\theta,\phi}$ at $t = 2T_{\mathrm{OAT}}$ immediately before BS2, with the best spin squeezing ξ achieved by optimizing θ and ϕ in the unitary $\hat{U}_{\theta,\phi}$ for BS2. The BEC's evolution between pulses approximately corresponds to OAT Hamiltonian $\hat{H}_{\mathrm{OAT}}(t) = \hbar\chi(t)\hat{j}_z^2$, where $\hat{j}_z = \frac{1}{2}(\hat{a}_1^\dagger\hat{a}_1 - \hat{a}_2^\dagger\hat{a}_2)$, $\chi(t) = \chi_{11}(t) + \chi_{22}(t) - 2\chi_{12}(t)$, and $\chi_{ij}(t) = (g_{ij}/2\hbar)\int d\mathbf{r}|u_i(\mathbf{r},t)|^2|u_j(\mathbf{r},t)|^2$, with $g_{ij} = 4\pi\hbar^2 a_{ij}/m$ and s-wave scattering lengths a_{ij} [74].

In the linear squeezing regime, the minimum spin squeezing is [74]

$$\xi^2 \approx \frac{1 - \frac{1}{2}|\mathcal{Q}|N\lambda(\sqrt{4 + |\mathcal{Q}|^2N^2\lambda^2} - |\mathcal{Q}|N\lambda)}{|\mathcal{Q}|^2}, \qquad (3)$$

where $\lambda \equiv \int_0^{2T_{\mathrm{OAT}}} dt'\chi(t')$ and $\mathcal{Q} \equiv |\mathcal{Q}|e^{i\varphi} = \int d\mathbf{r}u_1^*(\mathbf{r}, 2T_{\mathrm{OAT}})u_2(\mathbf{r}, 2T_{\mathrm{OAT}})$. Physically, $|\mathcal{Q}|$ quantifies how well the interferometer modes $\hat{a}_1$ and $\hat{a}_2$ are spatially matched at BS2 ($t = 2T_{\mathrm{OAT}}$), with $|\mathcal{Q}| = 1$ indicating perfect spatial overlap. Minimum spin squeezing requires $\theta \approx (3\pi/2) - \frac{1}{2}\tan^{-1}[2/(N|\mathcal{Q}|\lambda)]$ and $\phi = -\varphi$ for the BS2 unitary. Since $\lambda > 0$, Eq. (3) shows that $\xi < 1$ always, provided good mode overlap $|\mathcal{Q}|$ is maintained.

We estimate $\mathcal{Q}$ and λ by numerically solving the two-component Gross-Pitaevskii equation (GPE) for mean-field wave functions $\Psi_i(\mathbf{r},t)$ and identifying $u_i(\mathbf{r},t) = \Psi_i(\mathbf{r},t)/\sqrt{N}$ [74]. For concreteness, we take $|1\rangle$ and $|2\rangle$ as the $|F=1, m_F=0\rangle$ and $|F=2, m_F=0\rangle$ hyperfine states, respectively, of ^{87}Rb with $(a_{11}, a_{22}, a_{12}) = (100.4, 95.0, 97.66)a_0$ and $k_0 = 2k_L = 1.61 \times 10^7\,\mathrm{m}^{-1}$ (780 nm D2 transition). Figure 2 illustrates the key advantages of our scheme by plotting how $\chi(t)$, $\lambda(t) = \int_0^t dt'\chi(t')$ and $|\mathcal{Q}(t)| = |\int d\mathbf{r}u_1^*(\mathbf{r},t)u_2(\mathbf{r},t)|$ vary during the interferometer sequence. All three scattering lengths are of similar magnitude, so during the short duration where the two modes are strongly overlapped, $\chi(t)$ is almost zero and little spin squeezing is produced. However, the two modes rapidly separate ($\sim$1 ms) whilst the interatomic interactions are still significant, substantially increasing $\lambda(t)$. Most of this increase occurs over the next 10 ms; after this, free expansion rapidly reduces the collisional energy and therefore $\chi(t)$. Fortunately, this expansion is self-similar, largely preserving the mode shape, allowing high spatial-mode overlap ($|\mathcal{Q}| \sim 1$) at the interferometer output.

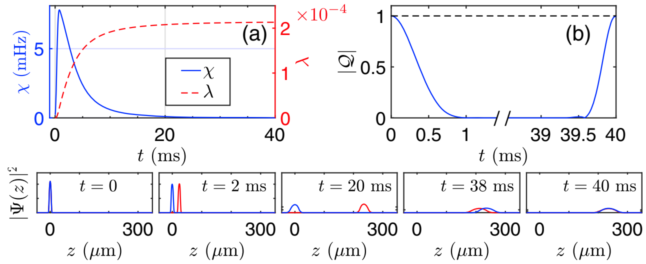

FIG. 2. Analytic spin squeezing model parameters determined from a GPE simulation of our scheme up to $t = 2T_{\mathrm{OAT}}$, with $T_{\mathrm{OAT}} = 20$ ms and an $N = 10^4$ atom BEC initially prepared in a spherical harmonic trap of frequency 50 Hz. (a) Effective squeezing rate $\chi(t)$ (blue, solid) and squeezing degree $\lambda(t)$ (orange, dashed). (b) Mode overlap $|\mathcal{Q}(t)|$. (Bottom) Normalized density slices at radial coordinate $r = 0$.

Spin squeezing results.—Although this analytic model provides qualitative insights into our scheme's viability, quantitative modeling requires a multimode description that, unlike the GPE, incorporates the effect of quantum fluctuations. This description is provided by the truncated Wigner (TW) method, which has successfully modeled BEC dynamics in regimes where nonclassical particle correlations become important [76,77,89–95]. In this approach, the BEC dynamics are efficiently simulated by a set of stochastic differential equations (SDEs), with averages over the solutions of these SDEs corresponding to symmetically ordered operator expectations [74].

Figure 3 compares the spin squeezing parameter computed from our analytic model Eq. (3), with λ and $|\mathcal{Q}|$ determined from 3D GPE simulations, to a direct computation of ξ via 3D TW simulations. We consider two scenarios: an initial spherical BEC prepared in a spherical harmonic trap of frequency 50 Hz [Fig. 3(a)] and an initial "pancake" BEC prepared in a cylindrically symmetric harmonic trap with frequencies $(f_r, f_z) = (32, 160)$ Hz in the radial and z directions [Fig. 3(b)]. Although the analytic model correctly captures the atom-number dependence, it overestimates the degree of squeezing by roughly a factor of two. An exception is for the largest atom numbers considered in the spherical case, where TW predicts much worse squeezing. For these atom numbers, the interatomic interactions are sufficiently strong such that intercomponent scattering strongly degrades the mode overlap, even though the clouds are initially overlapped for only $\sim$1 ms [Figs. 3(e) and 3(f)]. This is not seen in the GPE simulations [Figs. 3(c) and 3(d)] which neglect spontaneous scattering processes that clearly matter. In contrast, for an initially pancake-shaped BEC that is spatially tight in z, the two modes spatially separate on a timescale much faster than the spherical case. This mitigates the effect interatomic interactions have on mode matching

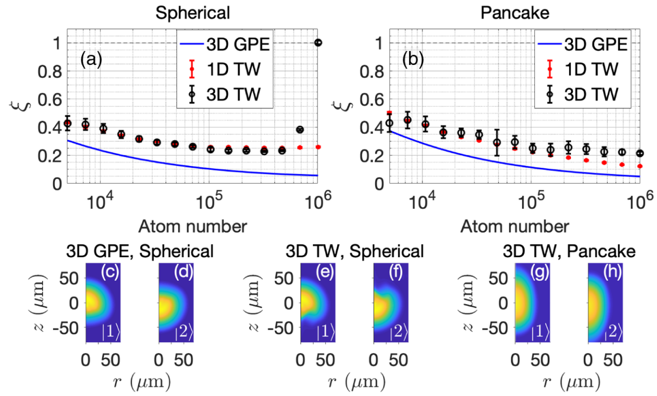

FIG. 3. Minimum spin squeezing parameter ξ for $T_{\mathrm{OAT}} = 10$ ms and atom number N [74]. In (a) the BEC is initially prepared in a spherical harmonic trap ($f_r = f_z = 50$ Hz), whereas in (b) an initial "pancake" BEC is prepared in a cylindrically symmetric harmonic trap ($f_r = 32$ Hz, $f_z = 160$ Hz). TW simulations are compared to Eq. (3) with model parameters determined from GPE simulations ("3D GPE"). (c)–(h) Density profiles for $N = 10^6$ at $t = 2T_{\mathrm{OAT}}$. The analytic model fails here for the spherical BEC case since spontaneous scattering degrades mode overlap.

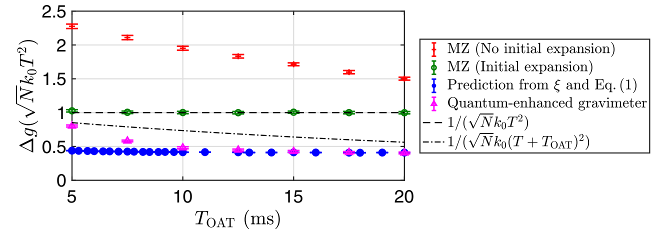

FIG. 4. One-dimensional TW calculations of sensitivity Δg for an $N = 10^4$ atom BEC initially prepared in a cylindrically symmetric harmonic trap ($f_r = 32$ Hz, $f_z = 160$ Hz). From top to bottom: (red) MZ with total interrogation time $T + T_{\mathrm{OAT}}$ (no initial period of free expansion), (green) BEC undergoes free expansion for duration $2T_{\mathrm{OAT}}$, followed by MZ of interrogation time T [Fig. 1(a)]; (magenta) quantum-enhanced BEC gravimetry [Fig. 1(b)]; (blue) Eq. (1) with ξ computed via TW. All four cases have the same total duration $2(T_{\mathrm{OAT}} + T)$ with $T = 60$ ms. The SNL for an ideal MZ of interrogation time T (dashed) and $T + T_{\mathrm{OAT}}$ (dot dashed) are marked for comparison. Our quantum-enhanced scheme always outperforms MZ schemes, even when phase diffusion is non-negligible.

[Figs. 3(g) and 3(h)], allowing significant squeezing even for $N = 10^6$ atoms.

Simulation of full interferometer sequence.—Although the spin squeezing parameter shows that our scheme produces significant spin squeezing, it does not confirm that this spin squeezing leads to a more sensitive measurement of g. Residual interatomic interactions may further degrade mode overlap during the remainder of the interferometer sequence and can couple to quantum fluctuations in $\hat{J}_z$, causing phase diffusion [67,68]. Both effects may degrade the sensitivity from the value predicted by Eq. (1). We confirm that these effects are not significant in our scheme by simulating the full interferometer sequence and directly computing the sensitivity via $\Delta g^2 = \mathrm{Var}(\hat{J}_z)/(\partial\langle\hat{J}_z\rangle/\partial g)^2$. 3D TW simulations of the full interferometer sequence are computationally infeasible, since they require prohibitively large grids and numbers of trajectories. Instead, we use an effective 1D TW model for these simulations, which assumes a Thomas-Fermi radial profile that self-similarly expands according to scaling solutions [74]. As shown in Fig. 3, this model perfectly agrees with 3D TW simulations except for the largest atom numbers.

Our scheme's sensitivity for an initial pancake BEC of $N = 10^4$ atoms and $T = 60$ ms is shown in Fig. 4. Although phase diffusion degrades the sensitivity for small T_{OAT}, its effect rapidly reduces for increasing T_{OAT}, becoming negligible for $T_{\mathrm{OAT}} \gtrsim 15$ ms. We compare our scheme to two SNL cold-atom gravimeters with the same initial BEC and total interferometer time $2(T_{\mathrm{OAT}} + T)$: (1) the conventional BEC gravimeter depicted in Fig. 1(a) (MZ with initial $T_{\mathrm{exp}} = 2T_{\mathrm{OAT}}$ period of free expansion) and (2) a MZ with no initial period of free expansion, thereby having an increased interrogation time $T + T_{\mathrm{OAT}}$. As expected, the former has negligible phase diffusion, attaining the ideal SNL result $\Delta g = 1/(\sqrt{N}k_0T^2)$. The latter suffers from considerable phase diffusion, far outweighing the benefit of increased interrogation time. Our scheme outperforms both SNL gravimeters, demonstrating the clear benefit of using the initial $2T_{\mathrm{OAT}}$ period to produce spin squeezing.

Experimental imperfections.—Finally, we assess the effect of three common experimental imperfections.

(1) Shot-to-shot fluctuations in laser intensity: although the laser pulse intensity is stable during a single interferometer run, it can vary between experimental runs [96]. Such shot-to-shot intensity fluctuations cause an offset $\delta\theta$ to the angle of all beam splitters and mirrors in that run, where $\delta\theta$ varies from shot to shot [50]. To first order, $\delta\theta \approx 2\Delta f$, where Δf is the fractional change in the population ratio due to imperfect beam splitting (e.g., $\Delta f = 0.02$ means that a 50/50 beam splitter is instead performed as a 48/52 beam splitter). We simulated the full interferometer sequence assuming that all five laser pulses suffered from Gaussian-distributed shot-to-shot fluctuations $\delta\theta$ of variance σ_θ^2. As shown in Fig. 5(a), these shot-to-shot fluctuations have a relatively small effect on Δg, since common rotation errors from the different pulses largely cancel.

(2) Shot-to-shot fluctuations in atom number: the optimal rotation angle θ for BS2 depends on the atom number. This cannot be known precisely and varies 10%–20% for different experimental runs [7,62]. Consequently, θ will deviate from the optimum from shot to shot, degrading ξ. We quantify this by assuming Gaussian-distributed shot-to-shot atom number fluctuations

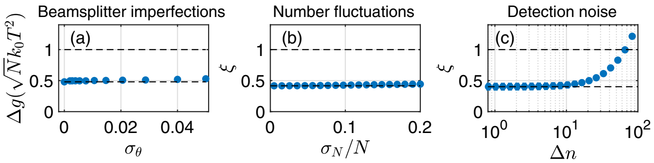

FIG. 5. The effect on our scheme of (a) Gaussian shot-to-shot beam splitting angle fluctuations of variance σ_θ^2, (b) Gaussian shot-to-shot atom-number fluctuations of variance σ_N^2, and (c) imperfect atom detection of resolution Δn. Here $N = 10^4$, $T_{\mathrm{OAT}} = 10$ ms, with an initial BEC prepared in a cylindrically symmetric harmonic trap ($f_r = 32$ Hz, $f_z = 160$ Hz). In (a) the sensitivity was obtained via 1D TW simulations of the full interferometer ($T = 60$ ms), whereas (b) and (c) computed the spin squeezing parameter from 3D TW simulations.

about mean N with variance σ_N^2. To leading order, optimal BS2 parameters for atom number N give $\xi(\sigma_N) \lesssim \xi + [1/(2|\mathcal{Q}|^2)](\sigma_N/N)^2$ [74], so shot-to-shot atom number fluctuations weakly impact the spin squeezing. This is confirmed by TW simulations [Fig. 5(b)].

(3) Imperfect atom detection: we model imperfect detection resolution as a Gaussian noise of variance $(\Delta n)^2$, corresponding to uncertainty Δn in the measured atom number. Imperfect detection increases the variance in $\hat{J}_z$, giving poorer sensitivity $\Delta g^2 = [\mathrm{Var}(\hat{J}_z) + \Delta j_z^2)]/(\partial\langle\hat{J}_z\rangle/\partial g)^2$, where $\Delta j_z = \Delta n/\sqrt{2}$. Then Δg is given by Eq. (1) with a modified spin squeezing parameter $\xi(\Delta n)^2 \approx \xi^2 + (2/N)\Delta n^2$ [97]. Figure 5(a) plots the dependence of ξ on Δn. Although the requirements are stringent, they are achievable and comparable to other spin-squeezing experiments. For example, Ref. [98] reports $\Delta n \sim 8$ for an $N = 5 \times 10^5$ atom ensemble, which would minimally impact our scheme's sensitivity.

Conclusions.—We have presented a scheme for quantum-enhanced gravimetry that exploits a BEC's inherently strong interatomic interactions, rather than simply removing them through an initial free expansion period. This scheme allows high-precision gravimetry up to a factor of five below the SNL and is robust to a range of experimental imperfections. Concretely, a quantum-enhanced gravimeter with $N = 10^6$ and $\xi = 0.2$ is equivalent to a SNL gravimeter with $N = 2.5 \times 10^7$—a challenging atom number to attain with current cooling methods [65]. Equivalently, for a fixed sensitivity, $\xi = 0.2$ allows a fivefold reduction in device size, enabling the more compact gravimeters needed for low-SWAP scenarios. Larger values of k_0, obtainable via Bragg pulses [5], could reduce the initial period of time where the two modes are overlapping. This would further reduce the deleterious effect of spontaneous scattering at large N, potentially allowing more significant degrees of spin squeezing. Since our proposal operates in free space, requiring only a small modification to existing laboratory setups, it provides a path towards realizing quantum-enhanced cold-atom gravimetry in the immediate future.

We acknowledge fruitful discussions with Chris Freier, Kyle Hardman, Joseph Hope, Nicholas Robins, and Paul Wigley. This project was partially funded by a Defence Science and Technology Group Competitive Evaluation Research Agreement, Project MyIP: 7333. S. S. S. was supported by an Australian Research Council Discovery Early Career Researcher Award (DECRA), Project No. DE200100495. S. P. N. acknowledges funding from the H2020 QuantERA ERA-NET Cofund in Quantum Technologies, project CEBBEC. This research was undertaken with the assistance of resources and services from the National Computational Infrastructure (NCI), which is supported by the Australian Government.

*stuart.szigeti@anu.edu.au

[1] A. Peters, K. Y. Chung, and S. Chu, Measurement of gravitational acceleration by dropping atoms, Nature (London) **400**, 849 (1999).
[2] A. Peters, K. Y. Chung, and S. Chu, High-precision gravity measurements using atom interferometry, Metrologia **38**, 25 (2001).
[3] Z.-K. Hu, B.-L. Sun, X.-C. Duan, M.-K. Zhou, L.-L. Chen, S. Zhan, Q.-Z. Zhang, and J. Luo, Demonstration of an ultrahigh-sensitivity atom-interferometry absolute gravimeter, Phys. Rev. A **88**, 043610 (2013).
[4] M. Hauth, C. Freier, V. Schkolnik, A. Senger, M. Schmidt, and A. Peters, First gravity measurements using the mobile atom interferometer gain, Appl. Phys. B **113**, 49 (2013).
[5] P. A. Altin, M. T. Johnsson, V. Negnevitsky, G. R. Dennis, R. P. Anderson, J. E. Debs, S. S. Szigeti, K. S. Hardman, S. Bennetts, G. D. McDonald, L. D. Turner, J. D. Close, and N. P. Robins, Precision atomic gravimeter based on Bragg diffraction, New J. Phys. **15**, 023009 (2013).
[6] C. Freier, M. Hauth, V. Schkolnik, B. Leykauf, M. Schilling, H. Wziontek, H.-G. Scherneck, J. Müller, and A. Peters, Mobile quantum gravity sensor with unprecedented stability, J. Phys. Conf. Ser. **723**, 012050 (2016).
[7] K. S. Hardman, P. J. Everitt, G. D. McDonald, P. Manju, P. B. Wigley, M. A. Sooriyabandara, C. C. N. Kuhn, J. E. Debs, J. D. Close, and N. P. Robins, Simultaneous Precision Gravimetry and Magnetic Gradiometry with a Bose-Einstein Condensate: A High Precision, Quantum Sensor, Phys. Rev. Lett. **117**, 138501 (2016).
[8] M. J. Snadden, J. M. McGuirk, P. Bouyer, K. G. Haritos, and M. A. Kasevich, Measurement of the Earth's Gravity Gradient with an Atom Interferometer-Based Gravity Gradiometer, Phys. Rev. Lett. **81**, 971 (1998).
[9] G. Stern, B. Battelier, R. Geiger, G. Varoquaux, A. Villing, F. Moron, O. Carraz, N. Zahzam, Y. Bidel, W. Chaibi, F. Pereira Dos Santos, A. Bresson, A. Landragin, and P. Bouyer, Light-pulse atom interferometry in microgravity, Eur. Phys. J. D **53**, 353 (2009).
[10] F. Sorrentino, Q. Bodart, L. Cacciapuoti, Y.-H. Lien, M. Prevedelli, G. Rosi, L. Salvi, and G. M. Tino, Sensitivity limits of a raman atom interferometer as a gravity gradiometer, Phys. Rev. A **89**, 023607 (2014).
[11] G. W. Biedermann, X. Wu, L. Deslauriers, S. Roy, C. Mahadeswaraswamy, and M. A. Kasevich, Testing gravity

with cold-atom interferometers, Phys. Rev. A **91**, 033629 (2015).

[12] G. D'Amico, F. Borselli, L. Cacciapuoti, M. Prevedelli, G. Rosi, F. Sorrentino, and G. M. Tino, Bragg interferometer for gravity gradient measurements, Phys. Rev. A **93**, 063628 (2016).

[13] P. Asenbaum, C. Overstreet, T. Kovachy, D. D. Brown, J. M. Hogan, and M. A. Kasevich, Phase Shift in an Atom Interferometer Due to Spacetime Curvature Across Its Wave Function, Phys. Rev. Lett. **118**, 183602 (2017).

[14] K. Bongs, M. Holynski, J. Vovrosh, P. Bouyer, G. Condon, E. Rasel, C. Schubert, W. P. Schleich, and A. Roura, Taking atom interferometric quantum sensors from the laboratory to real-world applications, Nat. Rev. Phys. **1**, 731 (2019).

[15] C. Jekeli, Navigation error analysis of atom interferometer inertial sensor, Navigation **52**, 1 (2005).

[16] B. Battelier, B. Barrett, L. Fouche, L. Chichet, L. Antoni-Micollier, H. Porte, F. Napolitano, J. Lautier, A. Landragin, and P. Bouyer, Development of compact cold-atom sensors for inertial navigation, in *Quantum Optics*, Vol. 9900, edited by J. Stuhler and A. J. Shields, International Society for Optics and Photonics (SPIE, Brussels, 2016), pp. 21–37.

[17] P. Cheiney, L. Fouché, S. Templier, F. Napolitano, B. Battelier, P. Bouyer, and B. Barrett, Navigation-Compatible Hybrid Quantum Accelerometer Using a Kalman Filter, Phys. Rev. Applied **10**, 034030 (2018).

[18] E. H. van Leeuwen, BHP develops airborne gravity gradiometer for mineral exploration, Leading Edge **19**, 1296 (2000).

[19] R. Geiger, V. Ménoret, G. Stern, N. Zahzam, P. Cheinet, B. Battelier, A. Villing, F. Moron, M. Lours, Y. Bidel, A. Bresson, A. Landragin, and P. Bouyer, Detecting inertial effects with airborne matter-wave interferometry, Nat. Commun. **2**, 474 (2011).

[20] M. I. Evstifeev, The state of the art in the development of onboard gravity gradiometers, Gyroscopy Navig. **8**, 68 (2017).

[21] B. Canuel *et al.*, Exploring gravity with the miga large scale atom interferometer, Sci. Rep. **8**, 14064 (2018).

[22] G. M. Tino *et al.*, Precision gravity tests with atom interferometry in space, Nucl. Phys. **B243-B244**, 203 (2013).

[23] O. Carraz, C. Siemes, L. Massotti, R. Haagmans, and P. Silvestrin, A spaceborne gravity gradiometer concept based on cold atom interferometers for measuring Earth's gravity field, Microgravity Sci. Technol. **26**, 139 (2014).

[24] D. N. Aguilera *et al.*, STE-QUEST—Test of the universality of free fall using cold atom interferometry, Classical Quantum Gravity **31**, 115010 (2014).

[25] J. Williams, S. w. Chiow, N. Yu, and H. Müller, Quantum test of the equivalence principle and space-time aboard the International Space Station, New J. Phys. **18**, 025018 (2016).

[26] D. Becker *et al.*, Space-borne Bose-Einstein condensation for precision interferometry, Nature (London) **562**, 391 (2018).

[27] S. Dimopoulos, P. W. Graham, J. M. Hogan, and M. A. Kasevich, Testing General Relativity with Atom Interferometry, Phys. Rev. Lett. **98**, 111102 (2007).

[28] V. Ménoret, P. Vermeulen, N. Le Moigne, S. Bonvalot, P. Bouyer, A. Landragin, and B. Desruelle, Gravity measurements below $10^9 g$ with a transportable absolute quantum gravimeter, Sci. Rep. **8**, 12300 (2018).

[29] J. Lautier, L. Volodimer, T. Hardin, S. Merlet, M. Lours, F. Pereira Dos Santos, and A. Landragin, Hybridizing matter-wave and classical accelerometers, Appl. Phys. Lett. **105**, 144102 (2014).

[30] A. V. Rakholia, H. J. McGuinness, and G. W. Biedermann, Dual-Axis High-Data-Rate Atom Interferometer Via Cold Ensemble Exchange, Phys. Rev. Applied **2**, 054012 (2014).

[31] T. van Zoest *et al.*, Bose-Einstein condensation in microgravity, Science **328**, 1540 (2010).

[32] A. Hinton *et al.*, A portable magneto-optical trap with prospects for atom interferometry in civil engineering, Phil. Trans. R. Soc. A **375**, 20160238 (2017).

[33] P. B. Wigley, K. S. Hardman, C. Freier, P. J. Everitt, S. Legge, P. Manju, J. D. Close, and N. P. Robins, Readout-delay-free Bragg atom interferometry using overlapped spatial fringes, Phys. Rev. A **99**, 023615 (2019).

[34] J. Estève, C. Gross, A. Weller, S. Giovanazzi, and M. K. Oberthaler, Squeezing and entanglement in a Bose-Einstein condensate, Nature (London) **455**, 1216 (2008).

[35] J. Appel, P. J. Windpassinger, D. Oblak, U. B. Hoff, N. Kjærgaard, and E. S. Polzik, Mesoscopic atomic entanglement for precision measurements beyond the standard quantum limit, Proc. Natl. Acad. Sci. U.S.A. **106**, 10960 (2009).

[36] B. Lücke, M. Scherer, J. Kruse, L. Pezzé, F. Deuretzbacher, P. Hyllus, O. Topic, J. Peise, W. Ertmer, J. Arlt, L. Santos, A. Smerzi, and C. Klempt, Twin matter waves for interferometry beyond the classical limit, Science **334**, 773 (2011).

[37] C. D. Hamley, C. S. Gerving, T. M. Hoang, E. M. Bookjans, and M. S. Chapman, Spin-nematic squeezed vacuum in a quantum gas, Nat. Phys. **8**, 305 (2012).

[38] B. Lücke, J. Peise, G. Vitagliano, J. Arlt, L. Santos, G. Tóth, and C. Klempt, Detecting Multiparticle Entanglement of Dicke States, Phys. Rev. Lett. **112**, 155304 (2014).

[39] W. Muessel, H. Strobel, D. Linnemann, T. Zibold, B. Juliá-Díaz, and M. K. Oberthaler, Twist-and-turn spin squeezing in Bose-Einstein condensates, Phys. Rev. A **92**, 023603 (2015).

[40] K. Lange, J. Peise, B. Lücke, I. Kruse, G. Vitagliano, I. Apellaniz, M. Kleinmann, G. Tóth, and C. Klempt, Entanglement between two spatially separated atomic modes, Science **360**, 416 (2018).

[41] J. Hald, J. L. Sørensen, C. Schori, and E. S. Polzik, Spin Squeezed Atoms: A Macroscopic Entangled Ensemble Created by Light, Phys. Rev. Lett. **83**, 1319 (1999).

[42] I. D. Leroux, M. H. Schleier-Smith, and V. Vuletić, Implementation of Cavity Squeezing of a Collective Atomic Spin, Phys. Rev. Lett. **104**, 073602 (2010).

[43] M. H. Schleier-Smith, I. D. Leroux, and V. Vuletić, Squeezing the collective spin of a dilute atomic ensemble by cavity feedback, Phys. Rev. A **81**, 021804(R) (2010).

[44] R. J. Sewell, M. Koschorreck, M. Napolitano, B. Dubost, N. Behbood, and M. W. Mitchell, Magnetic Sensitivity Beyond the Projection Noise Limit by Spin Squeezing, Phys. Rev. Lett. **109**, 253605 (2012).

[45] W. Wasilewski, K. Jensen, H. Krauter, J. J. Renema, M. V. Balabas, and E. S. Polzik, Quantum Noise Limited and

Entanglement-Assisted Magnetometry, Phys. Rev. Lett. **104**, 133601 (2010).

[46] M. F. Riedel, P. Böhi, Y. Li, T. W. Hänsch, A. Sinatra, and P. Treutlein, Atom-chip-based generation of entanglement for quantum metrology, Nature (London) **464**, 1170 (2010).

[47] C. Gross, T. Zibold, E. Nicklas, J. Estève, and M. K. Oberthaler, Nonlinear atom interferometer surpasses classical precision limit, Nature (London) **464**, 1165 (2010).

[48] I. D. Leroux, M. H. Schleier-Smith, and V. Vuletić, Orientation-Dependent Entanglement Lifetime in a Squeezed Atomic Clock, Phys. Rev. Lett. **104**, 250801 (2010).

[49] M. H. Schleier-Smith, I. D. Leroux, and V. Vuletić, States of an Ensemble of Two-Level Atoms with Reduced Quantum Uncertainty, Phys. Rev. Lett. **104**, 073604 (2010).

[50] O. Hosten, N. J. Engelsen, R. Krishnakumar, and M. A. Kasevich, Measurement noise 100 times lower than the quantum-projection limit using entangled atoms, Nature (London) **529**, 505 (2016).

[51] I. Kruse, K. Lange, J. Peise, B. Lücke, L. Pezzè, J. Arlt, W. Ertmer, C. Lisdat, L. Santos, A. Smerzi, and C. Klempt, Improvement of an Atomic Clock Using Squeezed Vacuum, Phys. Rev. Lett. **117**, 143004 (2016).

[52] W. P. Schleich, D. M. Greenberger, and E. M. Rasel, Redshift Controversy in Atom Interferometry: Representation Dependence of the Origin of Phase Shift, Phys. Rev. Lett. **110**, 010401 (2013).

[53] M. Kritsotakis, S. S. Szigeti, J. A. Dunningham, and S. A. Haine, Optimal matter-wave gravimetry, Phys. Rev. A **98**, 023629 (2018).

[54] S. A. Haine, Information-Recycling Beam Splitters for Quantum Enhanced Atom Interferometry, Phys. Rev. Lett. **110**, 053002 (2013).

[55] S. S. Szigeti, B. Tonekaboni, Wing Yung S. Lau, S. N. Hood, and S. A. Haine, Squeezed-light-enhanced atom interferometry below the standard quantum limit, Phys. Rev. A **90**, 063630 (2014).

[56] L. Salvi, N. Poli, V. Vuletić, and G. M. Tino, Squeezing on Momentum States for Atom Interferometry, Phys. Rev. Lett. **120**, 033601 (2018).

[57] A. Shankar, L. Salvi, M. L. Chiofalo, N. Poli, and M. J. Holland, Squeezed state metrology with Bragg interferometers operating in a cavity, Quantum Sci. Technol. **4**, 045010 (2019).

[58] P. Hamilton, M. Jaffe, J. M. Brown, L. Maisenbacher, B. Estey, and H. Müller, Atom Interferometry in an Optical Cavity, Phys. Rev. Lett. **114**, 100405 (2015).

[59] M. Kitagawa and M. Ueda, Squeezed spin states, Phys. Rev. A **47**, 5138 (1993).

[60] A. Sørensen, L. M. Duan, J. I. Cirac, and P. Zoller, Many-particle entanglement with Bose-Einstein condensates, Nature (London) **409**, 63 (2001).

[61] M. Kasevich and S. Chu, Measurement of the gravitational acceleration of an atom with a light-pulse atom interferometer, Appl. Phys. B **54**, 321 (1992).

[62] K. S. Hardman, C. C. N. Kuhn, G. D. McDonald, J. E. Debs, S. Bennetts, J. D. Close, and N. P. Robins, Role of source coherence in atom interferometery, Phys. Rev. A **89**, 023626 (2014).

[63] J. E. Debs, P. A. Altin, T. H. Barter, D. Döring, G. R. Dennis, G. McDonald, R. P. Anderson, J. D. Close, and N. P. Robins, Cold-atom gravimetry with a Bose-Einstein condensate, Phys. Rev. A **84**, 033610 (2011).

[64] S. S. Szigeti, J. E. Debs, J. J. Hope, N. P. Robins, and J. D. Close, Why momentum width matters for atom interferometry with Bragg pulses, New J. Phys. **14**, 023009 (2012).

[65] N. P. Robins, P. A. Altin, J. E. Debs, and J. D. Close, Atom lasers: Production, properties and prospects for precision inertial measurement, Phys. Rep. **529**, 265 (2013).

[66] S. Abend, M. Gersemann, C. Schubert, D. Schlippert, E. M. Rasel, M. Zimmermann, M. A. Efremov, A. Roura, F. A. Narducci, and W. P. Schleich, Atom interferometry and its applications, in *Proceedings of the International School of Physics "Enrico Fermi"*, edited by W. P. Schleich, E. M. Rasel, and S. Wölk (IOS Press, Amsterdam, 2020), pp. 345–392.

[67] P. A. Altin, G. McDonald, D. Döring, J. E. Debs, T. H. Barter, J. D. Close, N. P. Robins, S. A. Haine, T. M. Hanna, and R. P. Anderson, Optically trapped atom interferometry using the clock transition of large 87 Rb Bose-Einstein condensates, New J. Phys. **13**, 065020 (2011).

[68] P. A. Altin, G. McDonald, D. Döring, J. E. Debs, T. H. Barter, N. P. Robins, J. D. Close, S. A. Haine, T. M. Hanna, and R. P. Anderson, Addendum to optically trapped atom interferometry using the clock transition of large 87 Rb Bose-Einstein condensates, New J. Phys. **13**, 119401 (2011).

[69] Y. Castin and R. Dum, Bose-Einstein Condensates in Time Dependent Traps, Phys. Rev. Lett. **77**, 5315 (1996).

[70] Yu. Kagan, E. L. Surkov, and G. V. Shlyapnikov, Evolution of a Bose-condensed gas under variations of the confining potential, Phys. Rev. A **54**, R1753 (1996).

[71] F. T. Arecchi, E. Courtens, R. Gilmore, and H. Thomas, Atomic coherent states in quantum optics, Phys. Rev. A **6**, 2211 (1972).

[72] G. S. Agarwal, State reconstruction for a collection of two-level systems, Phys. Rev. A **57**, 671 (1998).

[73] S. A. Haine, J. Lau, R. P. Anderson, and M. T. Johnsson, Self-induced spatial dynamics to enhance spin squeezing via one-axis twisting in a two-component Bose-Einstein condensate, Phys. Rev. A **90**, 023613 (2014).

[74] See the Supplemental Material at http://link.aps.org/supplemental/10.1103/PhysRevLett.125.100402, which includes Refs. [5,7,59,69,75–86], for derivations of Eq. (1) and analytic model [e.g.m Eq. (3)], the optimal BS2 parameters for Fig. 3, and numerical simulation details.

[75] S. A. Haine and J. J. Hope, A multi-mode model of a non-classical atom laser produced by outcoupling from a Bose-Einstein condensate with squeezed light, Laser Phys. Lett. **2**, 597 (2005).

[76] M. J. Steel, M. K. Olsen, L. I. Plimak, P. D. Drummond, S. M. Tan, M. J. Collett, D. F. Walls, and R. Graham, Dynamical quantum noise in trapped Bose-Einstein condensates, Phys. Rev. A **58**, 4824 (1998).

[77] A. Sinatra, C. Lobo, and Y. Castin, The truncated Wigner method for Bose-condensed gases: Limits of validity and applications, J. Phys. B **35**, 3599 (2002).

[78] G. R. Dennis, J. J. Hope, and M. T. Johnsson, Xmds2: Fast, scalable simulation of coupled stochastic partial differential equations, Comput. Phys. Commun. **184**, 201 (2013).

[79] M. L. Chiofalo, S. Succi, and M. P. Tosi, Ground state of trapped interacting Bose-Einstein condensates by an explicit imaginary-time algorithm, Phys. Rev. E **62**, 7438 (2000).

[80] P. B. Blakie, A. S. Bradley, M. J. Davis, R. J. Ballagh, and C. W. Gardiner, Dynamics and statistical mechanics of ultracold Bose gases using c-field techniques, Adv. Phys. **57**, 363 (2008).

[81] A. Polkovnikov, Phase space representation of quantum dynamics, Ann. Phys. (Amsterdam) **325**, 1790 (2010).

[82] B. Opanchuk and P. D. Drummond, Functional Wigner representation of quantum dynamics of Bose-Einstein condensate, J. Math. Phys. (N.Y.) **54**, 042107 (2013).

[83] D. F. Walls and G. J. Milburn, *Quantum Optics*, 2nd ed. (Springer-Verlag, Berlin and Heidelberg, 2008).

[84] C. W. Gardiner and P. Zoller, *Quantum Noise: A Handbook of Markovian and Non-Markovian Quantum Stochastic Methods with Applications to Quantum Optics*, 3rd ed. (Springer, Berlin and Heidelberg, 2004).

[85] M. K. Olsen and A. S. Bradley, Numerical representation of quantum states in the positive-P and Wigner representations, Opt. Commun. **282**, 3924 (2009).

[86] A. Sinatra, E. Witkowska, J.-C. Dornstetter, Yun Li, and Y. Castin, Limit of Spin Squeezing in Finite-Temperature Bose-Einstein Condensates, Phys. Rev. Lett. **107**, 060404 (2011).

[87] D. J. Wineland, J. J. Bollinger, W. M. Itano, and D. J. Heinzen, Squeezed atomic states and projection noise in spectroscopy, Phys. Rev. A **50**, 67 (1994).

[88] L. Pezzé and A. Smerzi, Entanglement, Nonlinear Dynamics, and the Heisenberg Limit, Phys. Rev. Lett. **102**, 100401 (2009).

[89] A. A. Norrie, R. J. Ballagh, and C. W. Gardiner, Quantum turbulence and correlations in Bose-Einstein condensate collisions, Phys. Rev. A **73**, 043617 (2006).

[90] B. Opanchuk, M. Egorov, S. Hoffmann, A. I. Sidorov, and P. D. Drummond, Quantum noise in three-dimensional BEC interferometry, Europhys. Lett. **97**, 50003 (2012).

[91] P. D. Drummond and B. Opanchuk, Truncated Wigner dynamics and conservation laws, Phys. Rev. A **96**, 043616 (2017).

[92] A. Johnson, S. S. Szigeti, M. Schemmer, and I. Bouchoule, Long-lived nonthermal states realized by atom losses in one-dimensional quasicondensates, Phys. Rev. A **96**, 013623 (2017).

[93] S. S. Szigeti, R. J. Lewis-Swan, and S. A. Haine, Pumped-Up SU(1,1) Interferometry, Phys. Rev. Lett. **118**, 150401 (2017).

[94] D. J. Brown, A. V. H. McPhail, D. H. White, D. Baillie, S. K. Ruddell, and M. D. Hoogerland, Thermalization, condensate growth, and defect formation in an out-of-equilibrium Bose gas, Phys. Rev. A **98**, 013606 (2018).

[95] S. A. Haine, Quantum noise in bright soliton matterwave interferometry, New J. Phys. **20**, 033009 (2018).

[96] R Karcher, A Imanaliev, S Merlet, and F Pereira Dos Santos, Improving the accuracy of atom interferometers with ultracold sources, New J. Phys. **20**, 113041 (2018).

[97] This assumes $\max_{\phi}\langle \hat{J}_{(\pi/2),\phi+(\pi/2)}\rangle = N/2$.

[98] N. J. Engelsen, R. Krishnakumar, O. Hosten, and M. A. Kasevich, Bell Correlations in Spin-Squeezed States of 500 000 Atoms, Phys. Rev. Lett. **118**, 140401 (2017).